DESERT

Desert
Online at http://desert.ut.ac.ir

Desert 20-1 (2015) 47-55

# Simulation of local scour caused by submerged horizontal jets with Flow-3D numerical model

M.A. Mehnifard[a], S. Dalfardi[b*], H. Baghdadi[c], Z. Seirfar[c]

[a] *Javid Institute of High Education, Jiroft, Iran*
[b] *Faculty of Natural Resources, Jiroft University of Agricultural Science and Natural Resources, Jiroft, Iran*
[c] *Consulting Engineer, Saze Ab Halil Co., Jiroft, Iran*

Received: 6 July 2014; Received in revised form: 30 September 2014; Accepted: 22 October 2014

**Abstract**

One of the most concerning issues for researchers is to predict the shape and dimensions of the scour pit near hydraulic structures such as the base of bridges, weirs, valves and stilling basins due to both financial and human hazards induced by destruction of the structure. As the scour issue has its own complexity in relation to the multiplicity of effecting factors on it, in this study therefore, the results of laboratory analysis of local scour due to submerged horizontal jets were compared with numerical simulation results from Flow-3D three-dimensional model to test the potency of the numerical model. As a result, the model is proposed in place of the experimental model which has its own drawbacks and high costs. In this study, we measure maximum scour depth in relative equilibrium in 2 states and 6 test modes with different valve openings and tail water depth per different discharges. Comparison of the results indicates about 11% error for Flow-3D numerical model in relation to the experimental model which by considering the complexity of scour and deposition phenomena, is considered a good result.

***Keywords***: Scouring; Horizontal drowned jet; Numerical model

## 1. Introduction

Scour phenomena is critical in structures as it is essential for it to be predicted before building any structure. This could jeopardize the stability of the structure, while the accumulation of eroded material with tail water elevation change will affect the output performance of the structure. However, one of the causes of scour is water jet, which is when a high speed fluid with low thickness enters into a lower speed liquid resulting in an interference field known as jet. If the jet is along the stream and exits in parallel with the erodible bed, while downstream water depth is higher than exiting jet thickness, it is called a "submerged horizontal jet". The flow output of some hydraulic structures results in downstream scour phenomena, such as the sliding valves which are in form of submerged horizontal jet. If this phenomenon extends beneath the foundation and around structures, it would lead to their destruction and sometimes, irreparable financial damage over time.

When it is so significant that it reaches the depth of foundation of river structures and endangers stability of such structures or results in their destruction, the importance of scour phenomena becomes evident. Moreover, accumulation of eroded materials may affect output performance of dams and structures through changing tail water level (Momeni, R., Momeni *et al*., 2006).

Local scour of submerged horizontal jet has been previously studied, and it was concluded that scour characteristics could be described by the time period to reach the equilibrium stage, the maximum erosion depth and sand mass of vertex positions. It was found that erosion rate was high mainly during the initial minutes and as the erosion continues, it becomes slower over time until reaching the equilibrium stage (Chatterjee and Ghosh, 1994).

* Corresponding author. Tel.: +98 34 43215585,
Fax: +98 34 43215587.
*E-mail address:* dalfardi.s@gmail.com

Scouring process downstream of a free falling jet was simulated into three-dimensional numerical simulation by using Flow-3D software package and k-ε standard model to model turbulence. Sediment type is non-cohesive with $D_{50}$ = 0.127 and two internal friction angles of 29º and 35º, which indicate loose and moderate density sediments, respectively. Dimensions of simulated scour pit were compared in a certain time interval, and it was suggested that the scour pit in the sediments with higher internal friction angle has downstream length, width, depth and height less than the sediments with lower internal friction angle (Amirasalani, 2008).

The extent of scour, sediments and flow movement pattern around the bases of bridges were studied using CFD three-dimensional model. Comparison of field measurements of scour depth and the results from the equations show that these equations often over-estimate the scour depth to some extent which can be explained by insufficient understanding of complex flow field around structures and weakness of numerical modes in solving complex flows (Marson *et al*., 2003).

Numerical 3D model studies on local scour were conducted with free surface by Lieu and Garcia (2008). They used VOF (volume of fluid) method to simulate free surface water flow and k-ε model for turbulence. Comparison of the numerical model results with the results of experimental model suggests the accuracy of the numerical method for predicting the scour.

Moreover, the effect of different lengths of beach scour resulting from horizontal submerged scour was studied by Mahboudi *et al*. (2010). Longitudinal profiles of downstream slide gate with non-adhesive scour materials; both unprotected and protected, were drafted and compared to each other in a beach. The obtained results showed that beaching could considerably lower scour (Mahboudi *et al*, 2010).

## 2. Material and methods

### *2.1. Experimental Model*

The physical model of the experiment is made of flume with a transparent plexiglass so that the changes could be seen in the profile of bed surface material. The flume dimensions are as follows: 8 m length; 25.5 cm width ; and 25 cm depth. The flume was adjusted to be perfectly horizontal and without slope. Furthermore, a sliding valve is placed in the flume in a way that the horizontal jet could be moved 25 cm on an apron after passing through the valve, and then meet erodible sediments to create scour profiles. Valve width is similar to flume width and its height is 30 cm as it could be move up and down on the wall of the flume to create different thickness horizontal jets. In order to control the water level in the flume (tail water depth), a control weir was used at the end of the flume. Materials and sediments used in the experiment are of uniform particle size with a diameter of 1 mm. The relative density of the particle ($\rho_s$) is 56/2 g per $cm^2$.

Figure 1 shows the physical model in the Laboratory (Agricultural Research Center, Tehran), where the positions of sliding valve and apron are shown

For the experiments, the sliding valve was leveled at its location and the jet thickness (valve opening) was also precisely set with tail water depth adjusted completely using a control weir. The experiments were performed in various scenarios with different discharges and tail water depths from which the results of scour depth were obtained. Figure 2 shows a schematic view of longitudinal scour profile formed at apron downstream at 0.25 m length caused by opening the sliding valve to the extent b m and horizontal water jet velocity of V (m/s).

### *2.2. Numerical model*

In flows with turbulence, time-averaged equations are used to include the effects of turbulence. Thus, the continuity equations and momentum equations (Reynolds) are used thus;

$$\frac{\partial u_i}{\partial x_i} = 0 \quad (1)$$

$$u_j \frac{\partial u_i}{\partial x_i} = -\frac{1}{\circ}\frac{\partial}{\partial x_i}\left(P\text{¢}ij + \circ u_i u_j\right) \quad (2)$$

where $\rho$ is fluid density, $u_j$ is velocity component of the flow with time mean, $P$ is dynamic pressure and $-\rho u_i u_j$ is turbulence stress. Turbulence stress is calculated with the Boussinesq date equation as follows:

$$-\circ\overline{u_i u_j} = \circ\nu_t + \left(\frac{\partial u_i}{\partial x_j} + \frac{\partial u_j}{\partial x_j}\right) - \frac{2}{3}k\text{¢}ij \quad (3)$$

In this paper, Flow-3D numerical model was used as a numerical model. The model is a powerful CFD software designed in support of research on dynamic behavior of liquids and gases in a wide range of applications. Flow-3D is designed especially for problems of one-, two- and three-dimensions and results are achieved in very little time in a steady state as the program is based on fundamental laws of mass, momentum and energy conservation for

application in various stages of flow in every field. In Flow-3D, free surface is modeled with the VOF technique. The software also uses the RNG model to model turbulent flow.

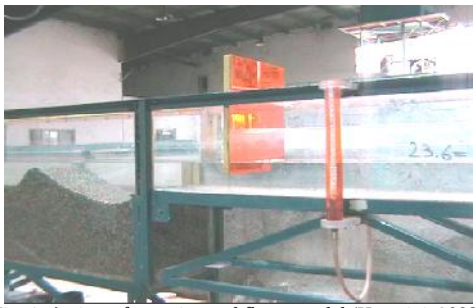

Fig. 1. A view of experimental flume model (Hosseini, 2008)

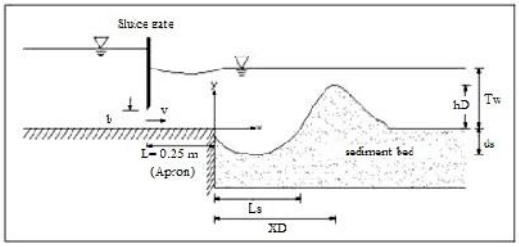


Fig. 2. A schematic view of longitudinal scour profile formed at apron downstream caused by submerged horizontal jet

One of the capabilities of Flow – 3D is that this software could choose a numerical solution as the final solution of a problem by meshing and solving unknown points in relation to known points. The smaller the mesh, the more accurate the results.. There are several numerical methods for solving problems. Flow-3D uses a simple grid of rectangular elements, so it has the advantages of ease of generation, regularity for improved numerical accuracy, and requires very little memory storage . Geometry within a grid is defined by calculating friction force areas and friction volume of each component. In the software, a motion equation is based on the finite volume technique.

Suspended sediments are in two forms:

1. The sediments are carried by local pressure gradient and become floating particles.
2. The deposited sediments are eroded. If the movement speed of floating and suspended sediments is much faster towards the deposited sediments than their erosion rate, they could be deposited.

Sediments concentration is expressed in units of grams per cubic centimeter. In the definition of concentration, deposits is represented by $f_s$ showing that the solid fraction represents the total volume of fluid and deposit. The liquid portion (water fluid) is represented by $f_l$.

$$f_L+f_s=1 \quad (4)$$

In this case, viscosity is calculated with the following formula:

$$\mu^* = \mu_r\left[1-\frac{\min(f_s, f_{s,o})}{f_{s,R}}\right]^{1.5} \quad (5)$$

where $\mu_f$ is molecular viscosity of the fluid, $\mu^*$ is the combined mean viscosity, and $f_{SCR}$ critical mass fraction. Macroscopic density is assumed as a linear function of the volume fraction of the sediments and is calculated based on the following formula:

$$\rho = \rho_L + f_s(\rho_s - \rho_L) \quad (6)$$

where $\rho_s$ and $\rho_L$ are densities of sediment and fluid particles, respectively. This model assumes that the sediment particles are spherical and the particle velocity is assumed to be small. Therefore, clearly the effects of viscosity are inevitable around each sediment particle. Therefore, the float factor is calculated as follows:

$$D_f = \frac{d_{50}^2\times(\rho_s-\rho_L)}{18\mu} \quad (7)$$

To calculate float factor, float rate is obtained as follows:

$$u_{drift} = D_f \times f_L \frac{\nabla p}{\rho} = \frac{f_L \times d_{50}^2}{18\mu}(\rho_s-\rho_L) \quad (8)$$

where D is average diameter of sediment particles, μ is viscosity of the fluid (water), and $\frac{\nabla P}{\rho}$ is body acceleration (sediment particles) which could be increased up to 10 times or more of gravity acceleration until the numerical pressure fluctuation effects disappear. Near the free surface of the fluid, is replaced by acceleration of gravity (g). In the flow areas where the solid (sediment) is filled, that is, its water fluid volume fraction is zero, floating rate tends to be zero from above. Shear stress of the deposited sediment bed results in movement of sediments. The amount of erosion that occurs on the surface of sedimentary deposits is a function of fluid shear stress, critical shear stress, density of the fluid and solid (sediment). One of the known conventional hydraulic deposition parameters is Shields critical parameter, a parameter which indicates the minimum shear stress required to lift a sediment particle from the sedimentary deposits bed.

$$\Theta_{crit} = \frac{\tau_{crit}}{g(\rho_f-\rho_s)d} \quad (9)$$

where $\tau_{crit}$ is minimum shear stress on the length of bed surface required to lift sediment particles. In this study, the model is used to predict sequential changes of sediment erosion at the local scale in relation to sedimentary deposits. The so called boundary layer velocity is shear velocity, which is expressed as $\sqrt{\tau/\rho}$. In all $u_{lift}$, $u_{drift}$ experimental models, the value of critical

shear velocity is to the extent that there would not be any erosion. Hence, the velocity required to lift sediments from sedimentary deposits bed is estimated based on a velocity higher than critical shear velocity which is expressed as $\sqrt{\frac{^2 - ^2_{crit}}{\sigma}}$. The formula below calculates lifting sediment from the sedimentary deposits bed surface which leads to scour.

$$U_{lift} = \sim n_s \sqrt{\frac{^2 - ^2_{crit}}{\sigma}} \quad (10)$$

where $n_s$ is normal vector of sedimentary deposits bed surface; α is a dimensionless parameter which indicates the probability of lifting sediment particles from the surface bed of sedimentary deposits, and is generally equal to or less than 1. Failure angle is another parameter included in this model.

$$\cdot\cdot = \frac{n_{\text{int}erface} . g}{|g|} \quad (11)$$

where $n_{interface}$ is normal surface vector and g is gravity acceleration vector . Failure angle determines how sharp the slope angle created by sedimentary deposits in a fixed flow area. When a hill or the projection of a soil type such as sand occurs, the failure angle is the same natural angle between the horizon and the hill.

In the sediment scour Flow-3D model, failure angle is represented by ¸ which is entered in unit of degrees as the modeling input in the software. The real failure angle, φ, is calculated by multiplying the normal vector. The model is applied by changing the critical shear stress at the gradient interface. Where φ is zero (i.e. a horizontal surface in relation to gravity). Effective critical shear stress is calculated by the following formula where $^2_{crit}$ is the critical shear stress.

$$^2_{crit} = ^2_{crit} \sqrt{\frac{1 - \sin^2 \cdot\cdot}{1 - \sin^2 ,}} \quad (12)$$

It is worth noting that when the local interface slope, φ, becomes equal to failure angle, ¸ , then $^2_{crit} = 0$. Overall, the model predicts negative values of $^2_{crit}$ where $\cdot\cdot > ,$ . In such a situation, sediments even in the absence of shear stress are itself eroded.

The movement of suspended sediments is described by the Advection - Diffusion equation in the considered system. Considering the total effects of floating and lifting sediments, the following equation is established.

$$\left(\frac{\partial c_s}{\partial t}\right)_x + u.\nabla c_s = D\nabla^2 c_s - u_{lift}.\nabla c_s - u_{drift}.\nabla c_s \quad (13)$$

Here u is the local fluid velocity, are the floating and lifting rates, respectively. Lifting rate is present everywhere except in the vicinity adjacent tothe sedimentary deposits interface, where the local shear stress is greater than $^2_{crit}$ . D is the diffusion coefficient which in Flow-3D is known as molecular diffusion coefficient.

As noted, Flow-3D utilizes regular rectangle grid to mesh. For meshing the model, the application of mesh system of Flow-3D software is illustrated in Table 1.

Table 1. Model meshing specifications

| Cannel three direction | Domail length (mm) | Cell no. |
|---|---|---|
| Length | 3000 | 500 |
| Width | 225 | 50 |
| Depth | 500 | 80 |

## 3. Results and discussion

### *3.1. Comparing depth of scour pit in numerical and experimental models.*

As the scour issue is highly complex due to the multiplicity of effecting factors, it is mostly studied in the laboratory. Since making a physical model requires a lot of resources and impossible in all situations, the use of a powerful numerical model could be key to obtaining good results spending less time and money. Therefore, this study aims to compare results of laboratory analysis of local scour caused by submerged horizontal jet with numerical simulation results of Flow-3D three dimensional model. To test potency of numerical model, the model is proposed in place of the experimental model in similar conditions.

The experimental model for the laboratory analysis was constructed in the Agricultural Soil and Water Research Center of Agriculture Jiahad Organization, Iran. After formulating the model at various tail water depths in relation to the values of physical model for two different conditions, the results of the model were compared with experimental results. In the first case, the valve was opened at 1 cm depth and 0.132 m tail water depth while in the second case, the valve was opened at 2 cm depth and 0.14 m tail water depth.

Figure 3 shows the graphical output of the two-dimensional model. The position of the sliding gate and the location of scour hole and bump (mound) are made visible.

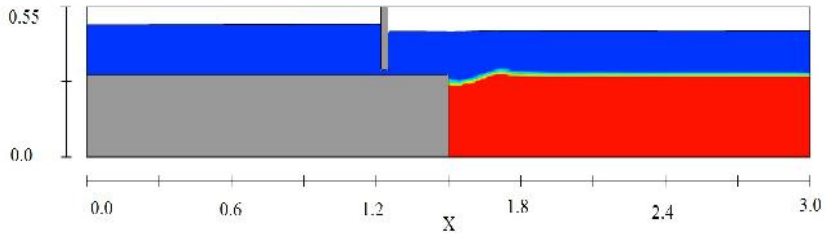


Fig. 3. A Plan of 2D graphical output of scour simulation results in Flow-3D numerical model

In the model, flow discharge, specified pressure with determined water level, Wall and Symmetry boundary conditions are considered for Woody boundary conditions, output, side walls and bed, and top boundary condition, respectively.

Important parameters affecting the results of the numerical model were calibrated and after matching the results with the results of the experimental model, the optimized parameters were applied to reduce errors in the simulation.

Also, after some modeling and comparison of the results, it was found that the turbulence model, RNG, provides better results in relation to other models and as such could be used in simulation.

Flow-3D numerical model results are compared with experimental model in Figure 4 for the first case and in Figure 5 for the latter. Also, Table 2 presents the error of Flow-3D numerical model in relation to the experimental model error. The average error rate of 6 tests in total is about 11%.

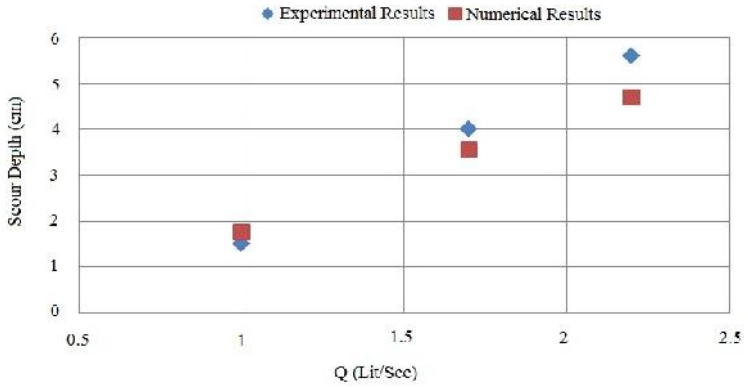


Fig. 4. Comparison of max scour depth results using experimental model and numerical model - First State [Numerical Results; Experimental Results; Scour depth (cm); Discharge (lit/s)]

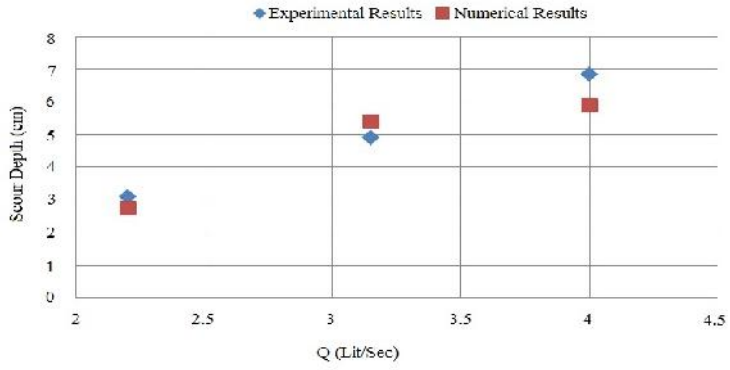


Fig. 5. Comparison of max scour depth results using experimental model and numerical model - Second State [Numerical Results; Experimental Results; Scour depth (cm); Discharge (lit/s)]

Table 2. Error of Flow-3D numerical model compared with experimental model

| | Discharge (lit/s) | Max depth of scour hole (cm) | | Error (%) |
|---|---|---|---|---|
| | | Experimental | Numerical | |
| First State | 1.00 | 1.50 | 1.70 | 11.8 |
| | 1.70 | 4.00 | 3.56 | 12.4 |
| | 2.20 | 5.60 | 4.90 | 14.3 |
| Second State | 2.20 | 3.10 | 2.80 | 10.7 |
| | 3.15 | 4.90 | 5.40 | 9.3 |
| | 4.00 | 6.85 | 6.10 | 12.3 |

### *3.2. Comparing Length of Scour Pit in Numerical and experimental Models*

Length of scour pit is the horizontal distance between bottom of the bed and scour profile intersection with the surface at downstream. In this study, scour pit length was measured in two states through the openings of gate (b) at different tailgate depths (Tw) and 2 sizes of grain (D50) equal to 1 and 3 mm at different discharge rates.

Table 3. Results of scour pit length in numerical and laboratory simulation along with error percentage compared to experimental model (3mm diameter)

| | Discharge (lit/s) | Length of scour hole (cm) | | Error (%) |
|---|---|---|---|---|
| | | Experimental | Numerical | |
| First State | 0.95 | 8.60 | 10.68 | 19.48 |
| | 1.70 | 17.70 | 19.42 | 8.86 |
| | 2.25 | 24.10 | 21.31 | 13.09 |
| Second State | 2.27 | 14.85 | 12.88 | 15.30 |
| | 3.21 | 22.30 | 24.54 | 9.13 |
| | 3.92 | 29.91 | 24.73 | 20.95 |

Table 4. Results of scour pit length in numerical and laboratory simulation along with error percentage compared to experimental model (3mm diameter)

| | Discharge (lit/s) | Length of scour hole (cm) | | Error (%) |
|---|---|---|---|---|
| | | Experimental | Numerical | |
| First State | 2.61 | 13.21 | 11.84 | 11.57 |
| | 3.21 | 17.57 | 14.68 | 19.69 |
| | 4.11 | 22.05 | 19.85 | 11.08 |
| Second State | 3.25 | 14.15 | 12.94 | 9.35 |
| | 4.60 | 20.31 | 23.65 | 14.12 |
| | 5.85 | 27.10 | 23.54 | 15.12 |

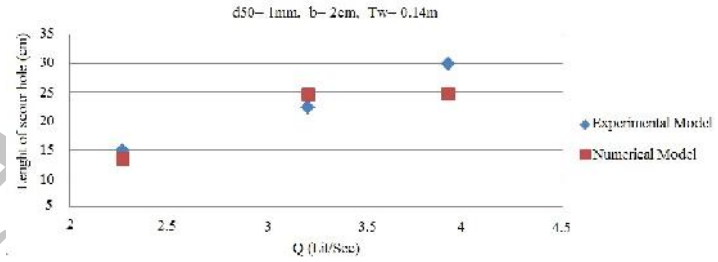


Fig. 6. Comparing scour pit length using experimental and numerical models of 1mm grain size

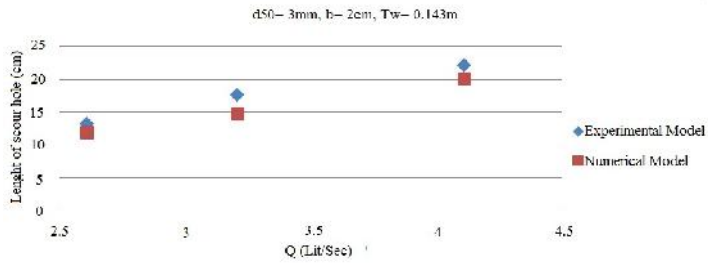


Fig. 7. Comparing scour pit length using experimental and numerical models of 3mm grain size

*3.3. Comparing height of scour pit downstream of the hump in numerical and experimental models.*

After scour pit formation, grains immediately initiate sedimentation which results in the formation of a hump at scour pit downstream. In this study, the height of scour pit hump downstream was measured in two states through the openings of gate (b) and different tailgate depths (Tw) and 2 sizes of grain (D50) equal to 1 and 3 mm at different discharge rates.

Table 5. Results of scour pit downstream hump height in numerical and laboratory simulations along with error percentage compared to experimental model (1mm diameter)

| | Discharge (lit/s) | Bulge height downstream scour hole (cm) | | Error (%) |
|---|---|---|---|---|
| | | Experimental | Numerical | |
| First State | 0.95 | 3.11 | 2.64 | 17.80 |
| | 1.70 | 6.64 | 5.25 | 26.48 |
| | 2.25 | 8.12 | 6.05 | 34.21 |
| Second State | 2.27 | 5.05 | 4.03 | 25.31 |
| | 3.21 | 7.25 | 6.04 | 20.03 |
| | 3.92 | 8.83 | 6.34 | 39.27 |

Table 6. Results of scour pit downstream hump height in numerical and laboratory simulations along with error percentage compared to experimental model (3mm diameter)

| | Discharge (lit/s) | Bulge height downstream scour hole (cm) | | Error (%) |
|---|---|---|---|---|
| | | Experimental | Numerical | |
| First State | 2.61 | 4.26 | 3.64 | 17.03 |
| | 3.21 | 6.23 | 5.23 | 19.12 |
| | 4.11 | 8.37 | 6.64 | 26.05 |
| Second State | 3.25 | 4.84 | 3.71 | 30.46 |
| | 4.60 | 7.68 | 6.84 | 12.28 |
| | 5.85 | 9.08 | 7.32 | 24.04 |

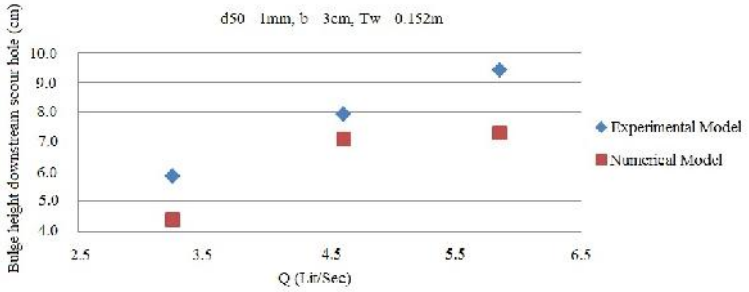


Fig. 8. Comparing scour pit downstream hump height using experimental and numerical models of 1 mm grain size

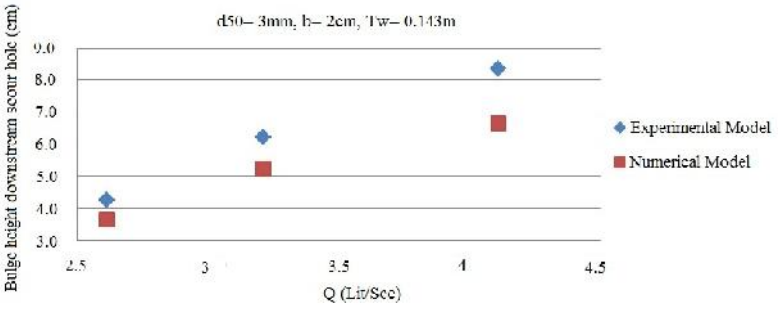


Fig. 9. Comparing scour pit downstream hump height using experimental and numerical models of 3 mm grain size

Results of this simulation were compared to experimental model and relative error between them is as follows:

- Mean relative error of scour pit depths between numerical and experimental models for diameters of 1 and 3 mm were 11.16 and 8.77, respectively.
- Mean relative error of scour pit length between the numerical and experimental models were obtained as 13.82 and 12.58, respectively, for diameters of 1 and 3 mm.
- Mean relative error of downstream hump height between the numerical and experimental models were 26.12 and 21.42, respectively for diameters of 1 and 3 mm.

Calculations were first carried out by applying the original scour model of FLOW-3D. Using default values for the critical sediment fraction (0.375) and cohesive sediment fraction (0.32), which were proposed by FLOW-3D for fine sand bed material, the numerical model did not reproduce the scour development with any acceptable quality.

A series of calculations were carried out with different model parameter sets to study their sensitivity on the numerical results. These results agree with that obtained by Abdelaziz *et al*. (2010).

Further calculations were done using the developed bed-load module. When a submerged jet flows over a sediment bed downstream of an apron, the local bed-shear stress induced by e high velocity of the jet exceeds the threshold bed-shear stress for the initiation of sediment motion which results in local scour downstream of the apron.

Furthermore, the study applied the developed module, FLOW-3D, to quantify the relationship among these factors. Hence, model tests were conducted for different efflux discharges q in the flume within thesame sand bed material. In the region above the jet, there is a large scale re-circulating region which extends downstream. It is important to recognize that this recirculation region provides for a significant downward velocity component downstream of the apron. This fits well qualitatively with the observations made in the experiment.

## 4. Conclusion

Scour hole depth is the most important parameter of the scour phenomenon. However, the importance of scour is evident when its depth becomes considerable and reaches the foundation of river structuresdeclining their stability or damaging them; that is, aggregation of eroded material could affect the performance of dams and hydraulic structures by changing tail water level. In this study, we measure d maximum scour depth in relative equilibrium at 2 states and 6 test modes with different valve openings and tail water depth per varying discharges. Comparison of the results indicates about 11% error for Flow-3D numerical model in relation to experimental model which in considering the complexity of scour and deposition phenomena, is considered a good result. Therefore, the problems and high costs of formulating/producing experimental models are avoided.

The turbulence model, RNG, provides better results compared to other turbulence models. By examining the results of the numerical simulations with the experimental model, the smallest error was observed in the calculation of maximum scour depth. In other words, in the numerical model Flow-3D, scour depth with accuracy better than other parameters are calculated.

In the simulations conducted, grain sizes of 3 mm diameter gave better results compared to 1 mm diameter. The main errors in test relating the calculation of scour pit downstream hump height is due to the grains assuming corners around by Flow-3D software. Rounded-corners slip over each other more frequently and this lowers hump height.

## References

Abdelaziz, S., M.D. Bui, P. Rutschmann, 2010. Numerical simulation of scour development due to submerged horizontal jet. River Flow. Process of the International Conference on Fluvial Hydraulics, 8–10 September, Braunschweig, Germany.

Ali Hosseini, P., 2008. The study of local scour due to submerged horizontal Jets using experimental models. M.Sc. Thesis, University of Tehran, Tehran, Iran.

Amir Aslani, Sh., M. Pirestani, A.A. Salehi neishabouri, 2008. Numerical study on the effects of internal friction angle of sediments on scour hole caused by free fall Jet. 2th National Conference on Dam and Hydroelectric Power Plants, 14&15 May, Tehran, Iran

Bakhiet, Sh., G.A. Abdel-Rahim, K.A. Ali, N. Izumi, 2013. Prediction of scour downstream regulators using ANNs. International Journal of Hydraulic Engineering, 2; 1-13.

Baranya S., J. Jozsa, 2006. Flow analysis in river danube by field measurement and 3D CFD turbulence modelling. Journal of Periodica Polytechnica. Civil Engineering, 50; 57–68.

Chatterjee, S., S. Ghoch, 1980. Submerged horizontal jet over erodible bed, Journal of the Hydraulics Division Proceedings of the American Society of Civil Engineers, 106; 1765-1782.

Day, S., A. Sarkar, 2008. Characteristics of turbulent flow in submerged jumps on rough beds. Journal of Engineering Mechanic, 134; 49-59.

Hager, W., H. Hans Erivin Minor, 2005. Plung pool in prototype and laboratory. Hydraulics of Dam and River structures, London, 165-172.

Hussein H.H, A.k.J. Inam, I.H. Nashwan, 2012. Evaluation of the local scour downstream untraditional bridge piers. Journal of Engineering and Development, 16; 36 – 49.

Hamidifar, H., M.H. Omid, M. Nasrabadi, 2011. Scour downstream of a rough rigid apron. World Applied Sciences Journal 14; 1169-1178.

Hopfinger, E.J., A. Kurniawan, W.H. Graf, W.U. Lemmin, 2004. Sediment erosion by gortler vortices: The scour-hole problem. Journal of Fluid Mechanics, 520; 327-342.

Karim, O.A., K.H.M. Ali, 2000. Prediction of patterns in local scour holes caused by turbulent water jets. Journal of Hydraulic Research, 38; 279-287.

Khanjani, M., M. Abdolahi, 2010. Numerical investigation of local scour and deposition of permeable breakwater. 8th International Seminar on River Engineering, 26-28January. Shahid Chamran University, Ahwaz, Iran.

Khosronejad, A., S. Kang, F. Sotiropoulos, 2012. Experimental and computational investigation of local scour around bridge piers. Journal of Advances in Water Resources, 37; 73-85.

Kim, Ch., J. Kang, H. Yeo, 2012. Experimental study on local scour in the downstream area of low drop structure types. Journal of Engineering, Scientific Research, 4; 459-466.

Mahboudi, A., J. Attari, M.R. Madjdzadeh tabatabai, 2010. Experimental study scour control of horizontal submerged jets using riprap. 5th National Congress on Civil Engineering, 4-6 May, Ferdowsi University of mashhad, Iran.

Marson, C., E. Caroni, V. Fiorotto, L. Deppo, 2003. Flow field analysis around a groin. Proc. of 30th IAHR Congress, Thessaloniki, Greece, Theme C, Hydraulics of Groynes, 377-384.

Mazurek, K., N. Rajaratnam, D. Sego, 2001. Scour of soil by submerged circular turbulent impinging jets. Journal of Hydraulic Engineering, 127; 598-606.

Momeni Vasalian, R., S.H. Mousavi Jahromi, M. Shafaei Bajestan, 2007. Scour rectangular jet downstream from the cup-shaped projectile. 7th International Seminar on River Engineering, 13-15 February, Shahid Chamran University, Ahwaz, Iran.

Najafzadeh, M., 2009, Experimental study and simulation of local scour at bridge foundations in cohesive soil. M.Sc. Thesis, Shahid Bahonar University, Kerman, Iran.

Nik Hassan, N., R. Narayanan, 1985. Local scour downstream of an apron. Journal of Hydraulic Engineering, 111; 1371-1385.

Pagliara, S., W. Hager, H. Minor, 2006. Hydraulic of plane pool scour. Journal of Hydraulic Engineering, 132; 450-461.

Salehi Neyshabouri A.A., A.M. Ferreira Da Silva, 2003. Numerical simulation of scour by a free falling jet. Journal of Hydraulic Research, 41; 533-539.

Smith,H. D B, 2007. Flow and sediment dynamics around three-dimensional structures in coastal environments. PhD thesis, The Ohio State University.

Sui, J., M.A.A. Faruque, R. Balachandar, 2008. Influence of channel width and tailwater depth on local scour caused by square jets. Journal of Hydro-environment Research , 2; 39-45.

Liu, X., M. García, 2008. Three - dimensional numerical model with free water surface and mesh deformation for local sediment scour. Journal of Waterway, Port, Coastal, and Ocean Engineering, ASCE, 134; 203–217.

Xianfan, C., Q. Yanlong, 2010. The numerical simulation of local scour around offshore pipeline. Proceedings of the Twentieth International Offshore and Polar Engineering Conference. Beijing, China, 20 – 25 June, e-book.lib.sjtu.edu.cn.